LA-UR- 10-00204

Approved for public release; distribution is unlimited.

Title: Description and Evaluation of the QUIC Bio-Slurry Scheme: Droplet Evaporation and Surface Deposition

Author(s): Dragan Zajic
Michael J. Brown
Matthew A. Nelson
Michael D. Williams

Intended for: 90th American Meteorological Society (AMS) Annual Meeting

Los Alamos NATIONAL LABORATORY
EST. 1943

Description and Evaluation of the QUIC Bio-Slurry Scheme: Droplet Evaporation and Surface Deposition

Dragan Zajic, Michael J. Brown, Matthew A. Nelson and Michael W. Williams
Los Alamos National Laboratory, Los Alamos, NM

1. Introduction

The Quick Urban and Industrial Complex (QUIC) model was developed with the goal of improving the transport and dispersion modeling capabilities within urban areas. The modeling system has the ability to quickly obtain a detailed 3D flow field around building clusters and uses a Lagrangian random-walk approach to calculate dispersion fields. When the pollutant is released into the atmosphere suspended within water droplets, the evaporation changes the droplet mass which then impacts its settling velocity. The evaporation rate depends on atmospheric conditions, e.g. relative humidity and temperature. In this paper we provide a description of the QUIC evaporation scheme and compare model's evaporation curves (diameter vs. time) with other models reported in the literature as well as experimental measurements of change in water droplet diameter with time for different temperatures and relative humidity. The QUIC is then applied to calculation of aerosol concentration, dosage and deposition fields and results are compared with results available in literature.

The bio-slurry option available within the QUIC modeling system enables calculations of dispersion of non-soluble agent suspended in water after it is emitted as droplet spray. The user specifies the amount of agent, the initial droplet size distribution, the concentration of solids in the solution (includes the bio agent itself plus other inert solids), the effective density of the dry agglomerate, the relative humidity and temperature of the air, and the atmospheric pressure. The droplets will evaporate with time as they move through the air while simultaneously being pulled downwards by gravity. When the water content is completely evaporated, a dry particle made up of biological agent and inert solids will be tracked. The size of the dry particle is determined by the initial concentration of solids in the solution and by the effective density of the dry agglomerate. The former determines the solids mass in each droplet and the latter provides an estimate of how tightly packed the biological agent (e.g., spores, cells) and inert solids are when dry. QUIC modeling system was tested and compared with other theoretical models as well as experimental measurements by Houghton (1933).

2. The QUIC evaporation scheme

The Quick Urban and Industrial Complex (QUIC) modeling system enables user to quickly obtain three-dimensional flow field and concentration and deposition contours in urban areas. Two major components of the modeling system are QUIC-Urb and QUIC Plume. QUIC-Urb calculates velocity field using empirically obtained flow parameterizations and imposes mass conservation while QUIC-Plume uses Lagrangian particle approach to calculate agent dispersion using previously obtained mean flow field and turbulence parameterization for different stability conditions. In recent years many additional capabilities were added to QUIC, including dense gas option, bio-slurry, QUIC-Pressure module etc.

Within bio-slurry option, the evaporation algorithm is enacted for marker particles i.e. water droplets having a radius larger than the minimum radius which is equal to the dry agglomerate particle radius (Williams et al. 2009). The time rate of change of the droplet radius r [m] due to evaporation is computed using:

$$\frac{dr}{dt} = \frac{D_{corr}(101325(P_v - P_d))}{(1\times 10^6 \rho) r\left(\frac{D_{corr} H_v (101325 P_d)\left(\frac{H_v}{RT} - 1\right)}{M_v k_{corr} T} + \frac{RT}{M_v}\right)}$$

where dr/dt is the time rate of change of the droplet radius [m/s], $Dcorr$ is the corrected diffusion coefficient of water vapor in air [m^2/s], Pv is the ambient water vapor pressure of the atmosphere [atm], Pd is the vapor pressure of water at the surface of the droplet [atm] (the factor of 101,325 converts both vapor pressures into Pascals), ρ is the density of liquid water [g/mL] (the factor of $1\text{x}10^6$ converts the density to g/m^3), Hv is the heat of vaporization of water [J/mol], R is the universal gas constant [8.314151 J/(molK)], T is the local atmospheric temperature [K], Mv is the molecular weight of water agent vapor [g/mol] and $kcorr$ is the corrected thermal conductivity of air [W/(mK)]. Below we show how each of these terms is computed.

To obtain $Dcorr$, the molecular diffusion coefficient D [m^2/s] is first computed based on Hall and Pruppacher (1976) and Pruppacher and Klett (1978):

$$D = 2.11 \times 10^{-5}\left(\frac{T}{T_0}\right)^{1.94}\left(\frac{P_0}{P}\right)$$

where T_0 is the reference air temperature [273.15 K], P_0 is the reference pressure [1 atm], T is the local air temperature [K], and P is the local pressure [atm]. The diffusion coefficient is then corrected for non-continuum effects through ventilation and collision geometry terms:

$$D_{corr} = D\frac{C_{vent}}{C_{coll}}.$$

The ventilation coefficient $Cvent$ is a function of the Reynolds number ($Re = Ud/v$) and the Schmidt number ($Sc = v/D$), where U is the droplet speed [m/s], d is the particle diameter [m], and ν is the kinematic viscosity of air [m^2/s]:

$$C_{vent} = 1 + 0.108 \mathrm{Re}\, Sc^{2/3} \qquad \text{for } \mathrm{Re}^{1/2} Sc^{1/3} \le 1.4$$

$$C_{vent} = 0.78 + 0.308 \mathrm{Re}^{1/2} Sc^{1/3} \qquad \text{for } \mathrm{Re}^{1/2} Sc^{1/3} > 1.4$$

The collision coefficient $Ccoll$ is a function of a geometry coefficient and a sticking coefficient:

$$C_{coll} = 1 + (C_{geom} + C_{stick})\frac{MFP}{r}$$

where

$$C_{geom} = 1.33 + \frac{0.70r/MFP}{1 + r/MFP}$$

and

$$C_{stick} = \frac{4 \cdot (1 - E_{stick})}{3E_{stick}}.$$

Here, r is the radius of the droplet [m], MFP is the mean free path of water in the vapor phase [m], and $Estick$ is the sticking efficiency [0-1]. For water vapor, the sticking efficiency is set to one.

The vapor pressure Pv of the ambient atmosphere is determined from the relative humidity profile and the saturation vapor pressure of water:

$$Pv(z) = rh(z) * Psat .$$

The saturation vapor pressure $Psat$ [atm] is computed using:

$$P_{sat} = P_{sat0} exp\left(\frac{M_v}{R}\left(A\left(\frac{T - T_0}{TT_0}\right) + Bln\left(\frac{T}{T_0}\right)\right)\right)$$

where $Psat0$ is the reference vapor pressure of water [6.03 X 10-3 atm], Mv is the molecular weight of water vapor [g/mol], R is the universal gas constant [8.314151 J/(molK)], T is the atmospheric temperature as function of height [K], $T0$ is the reference temperature [273.15 K], A has a value of 3.14839 X 103 J/g, and B has a value of 2.370 J/(gK).

The vapor pressure of water at the surface of the droplet Pd [atm] is

$$P_d = P_{sat} \exp\left[\frac{2\sigma M_{liq}}{rRT(1x10^6 \rho_{liq})}\right]$$

where σ is the surface tension of the water droplet [N/m], $Mliq$ is the molecular weight of liquid agent [g/mol], r is the radius of the droplet [m], and ρliq is the liquid density of the agent [g/mL] (the factor of $1X10^6$ converts the density to g/m3). The water droplet surface tension is calculated using:

$$\sigma = 0.001 \cdot (76.1 - 1.55(T - T_0)) \quad \text{if T} \geq \text{T}_0$$

$$\sigma = \sum_{i=1}^{7} \alpha_i (T - T_0)^i \quad \text{if T} < \text{T}_0$$

where $\alpha_1 = 7.593 \times 10^{-2}$, $\alpha_2 = 1.15 \times 10^{-4}$, $\alpha_3 = 6.818 \times 10^{-5}$, $\alpha_4 = 6.511 \times 10^{-6}$, $\alpha_5 = 2.933 \times 10^{-7}$, $\alpha_6 = 6.283 \times 10^{-9}$, and $\alpha_7 = 5.285 \times 10^{-11}$.

The heat of vaporization *Hv* [J/mol] is determined from

$$H_v = (2501 - 2.37 \cdot (T - T_0)) \cdot M_{liq}$$

while the corrected thermal conductivity of air *kcorr* [W/(mK)] is specified using:

$$k_{corr} = k \frac{C_{vent}}{C_{coll}}$$

where *Cvent* and *Ccoll* are as defined above with the exception of the Schmidt number, the mean free path of the agent vapor, and the sticking efficiency being replaced with the Prandtl number $Pr = \rho v C_p / k$, where C_p is the heat capacity of air [J/(kgK)]), the mean free path of air, and the thermal accommodation of air, respectively.

3. Evaporation curve comparisons

Houghton (1933) studied evaporation of fog drops which due to its low speed (<2 cm/s) can be considered stationary drops in still atmosphere. The measurements were conducted on drops at rest suspended from fine wires or glass filaments in the chamber where the humidity was kept constant. The diameter was measured using ocular micrometer in a low power microscope. The range of droplet sizes measured during the experiment was between 25 and 2600 microns and readings were taken from every 30 seconds to every ten minutes depending on the rate of evaporation. The results presented here (see Figures 1 and 2) show evaporation of droplets of initial size of approximately 500 microns and between 900 and 1000 microns at different temperatures and relative humidity. The QUIC-Plume calculations were performed for cases when the free falling velocity was taken into account as well as for zero speed ventilation. Since droplets in experiments were not in the state of the free fall, zero speed ventilation case is more appropriate comparison with experiment.

QUIC model was also compared with calculations of other theoretical models reported by Kukkonen et.al. (1989) and Morawska (2006). Kukkonen et.al. (1989) conducted theoretical study of evaporation of freely falling droplets of water and ammonia in gas mixtures containing air and evaporating gas vapor. The model numerically solves equations of mass and heat transfer from droplet surface including forced convection of mass and heat due to free fall. The gas temperature was 20°C and the vapor pressure in the gas was negligible.

Morawska (2006) reported calculations of droplet diameter change as a result of evaporation for three different initial droplet sizes (1, 10, and 100 microns) and for different relative humidity (RH). These results were used in studies of spread of infections. In this work we compared results for droplets of initial diameter 100 microns (Figure 3). Hinds (1999, 2001) developed evaporation model and calculated evaporation times for pure water droplets of different initial diameters at different relative humidity and temperature. We also calculated droplet evaporation times using QUIC model for the same conditions and compared the results.

Figures 1 and 2 show comparison of experimental results with QUIC calculations for different temperatures and relative humidity and for different initial droplet diameters. QUIC calculations for zero ventilation compare reasonably well for dry air although evaporation is slightly slower than during experiment. The less satisfactory performance occurred for the case of highest relative humidity RH=88% when the evaporation time is about 40% longer than value obtained from experiments.

For relative humidity in range from 0 to 60% QUIC evaporation scheme results are in a very good agreement with calculations of Kukkonen and Morawska (Figure 3) but for RH=80% evaporation is slightly faster for QUIC-Plume calculations.

Figure 4 shows comparison of drying times for different initial water droplet sizes at temperature 20 °C. In dry and humid air with relative humidity 50% there is a very good agreement between QUIC result and Hinds' calculations. For the case when relative humidity is 100 % the QUIC evaporation times are longer.

4. Deposition calculations

When the released material is dispersed through water droplets as in agricultural applications it is very important to have a good water evaporation scheme in order to correctly calculate dispersion and deposition of the material, although the rate of evaporation is not the only factor influencing the validity of deposition calculations

The field study results reported by Fritz and Hoffmann (2007) were used to validate QUIC deposition results. During this study the AirTractor AT-402B with aircraft spray boom was used to apply the spray solution consisted of water, Trition X-100 surfactant at 0.1% v/v, and Caracid Brilliant Flavine FFN fluorescent dye at 15 g/ha. The swath width was 20 m and height of application was 2.4 m above ground level. The nozzles were used to produce droplets of volume median diameter (VMD) of 236 microns. The percentage of spray volume contained in droplets less than 200 microns was 34%, while percentage of spray volume in droplets less than 100 microns was 14%. Meteorological conditions (wind speed and direction, temperature and humidity) were measured using the sensors placed on the tower 100 m downwind of the flight line at 2.5, 5 and 10 meters above the ground. These measurements enabled calculations of gradient Richardson number Ri which was reported as a measure of atmospheric thermal stability. The tower instruments measured one-minute averages of wind speed and direction (RM Young model 05701 Wind Monitor-RE), and temperature (RM Young model 43347VC Temperature Probes) at 2.5, 5, and 10 meters above the ground level. Relative humidity was measured with an RM Young model 71372 temperature/relative humidity sensor. Direction of flight line was normal to the wind speed (see Figure 5) and downwind sampling locations were located in the center of a large, (approx. 70 ha square) flat, field of wheat stubble 10 to 20 cm tall. Three sub-samples of mylar collectors at multiple downwind distances were used to measure spray deposition. Monofilament nylon screen cylinders positioned at multiple heights (0.3, 3, and 6 m) and downwind distances on sampling towers collected the airborne portion of the spray (Figure 5).

Table 1 provides information on atmospheric conditions during the performed tests and the QUIC simulation input was set to closely match the meteorological and spraying conditions during the selected field tests. Tables 2 and 3 give deposition measurement results reported by Fritz and Hoffmann (2007) given as a percentage of applied material. Deposition calculated by QUIC was calculated on horizontal uniform grid of size 10 m x 10 m and then calculated for different areas of interest (e.g. in-swath region and downwind regions of different sizes) so that it can be compared to measurement results reported in tables.

The first example presented here is the case number 9 (Rep 9 in table) where spraying was conducted at 7.36PM, atmospheric temperature was 33.5°C, relative humidity was 42.1% and wind speed at 2.5 m above ground level was 1.9 m/s. The gradient Richardson number calculated from measured wind speed and temperature was 0.081. Since the stability conditions in QUIC modeling system are set using the inverse Monin-Obukhov scale 1/L, the Ri value reported was converted to 1/L using the expression (Neumann 1961):

$$Ri = \frac{z}{L}\left(1 + \beta\frac{z}{L}\right).$$

where $\beta = -0.6$ and calculated value of 1/L is 0.047 1/m. This approximately corresponds to Pasquill's stability class E (Golder 1972, Arya 1999) assuming roughness length was between 1 and 2 cm which is about 10% of reported wheat stubble height. In order to represent the droplet size distribution as close as possible to experiment, the QUIC setup used lognormal size distribution with volume median diameter (VMD) and standard deviation (SD) set to 50 microns and 2.1, respectively. For these values the 54.6% of the volume is carried by droplet of size smaller than 236 microns while the volume fraction carried by droplets smaller than 100 and 200 microns is 12.1% and 44.4%, respectively. The source is represented as a rectangular box and different box sizes were used in attempt to account for influence of vortices created by the airplane wing. Since QUIC source definition module does not have ability to account for vortices created by wings we ran calculations for three different source sizes (see Figure 6). The source represented by the red line has dimensions 600 x 20 x 2.4 m (i.e. flight path length x boom width x height of the boom). For this source geometry we performed two set of calculations for neutral stability and stratified case (stable for case 9 and unstable for case 2) and named them QUIC 1 and QUIC 2 in legends of plots comparing model with experiment (Figures 7-9). The second source geometry used (blue dash line) is an attempt to include effects of wind induced vortices and expands the source height vertically and laterally. It is assumed that radius of the largest vortex is distance between ground and the wing which is approximately 2.4 m (boom height above the ground) and this value was used to extend dimensions of the source. Green line represents the third source shape with the same length and width as the first one but with different height (vertical dimension) of 0.1 m placed at the boom height level. Results for last two geometries are name QUIC 3 and QUIC 4 in comparison plots.

The other case simulated here is the case number 2, where spraying was conducted in the morning hours (7:43AM), when the temperature was 23°C, relative humidity was much higher than in the previous case (92.1%), wind speed was low 0.4 m/s and gradient Richardson number value of -0.77 indicates unstable thermal conditions. Conversion of Ri into 1/L fives value 1/L=-0.24 1/m which belongs to Pasquill stability class A. Since this value of inverse Monin-Obukhov length seems to be extreme for morning periods when sun heating of soil just started we also performed calculations for value of 1/L=-0.04 1/m which corresponds to stability class C. In this case, again, we conducted calculation for different source geometries and for neutral thermal stability.

Deposition was calculated within following regions (along-wind span): In-swath (-20-0 m just under source), 0-10m, 10-20m, 20-30m, 30-40m, 40-50m, 50-75m, 75-100m, 100-150m, 150-200m. Zero coordinate in the plots comparing experiments with models is at the downwind edge of the boom and downwind spatial coordinate is centered at the corresponding area where deposition is calculated. The regions spans laterally across the whole domain and each calculated deposited mass is normalized by the mass of released spray.

5. Deposition results and conclusions

Figures 7-9 show plots comparing experimental measurements with QUIC modeling results for four different simulation settings. For the case 9 (Figure 7) the in-swath calculated deposition masses are more than double the measured values. Modeled deposited mass change with distance is much steeper when compared to experiments so that after 10 m from source's downwind edge values are much lower then measured. In this region the best performing modeling results are for the case when the source is modeled as thin rectangular of vertical depth 0.1 m placed at boom height (simulation settings QUIC 4) and values are about the half of the measured values. Worst performance is for the neutral stability runs where the values are at least 4 times lower than field test results.

The case 2 characterized by much higher humidity and unstable conditions was simulated for two values of l/L and results are given in Figures 8 and 9. In both cases the in-swath deposition is close to measured value for all QUIC runs especially for neutral case (QUIC 1). QUIC deposition values again drop fast and downwind deposition is significantly lower than measured.

The reason for underestimation of deposited mass further downwind could be multiple, one of which is the difficulty to exactly incorporate influence of wing induced vortices which would increase the momentum of sprayed droplets and contribute to its downwind transport. For the case 2 when the relative humidity was high the reason for even larger discrepancy in downwind deposition could be due to shorter evaporation times of QUIC evaporation scheme when compared to experimental curves at higher humidity. The slower evaporation means heavier drops which then fall to the ground faster and don't reach far downwind. Also, there is a question how reliable is the information on input parameters e.g. the initial droplet size distribution or information on thermal stability. Also variability in wind speed and direction could influence transport of the sprayed material.

6. References

Arya S.P. Air Pollution Meteorology and Dispersion, Oxford University Press, 1999

Fritz B.K and Hoffmann W.C, Meteorological Influences on Mass Accountability of Aerially Applied Sprays, 2007 ASABE/NAAA Technical Session, 41st Annual National Agricultural Aviation Association Convention, Silver Legacy Resort, Reno, Nevada, December 10, 2007

Golder D., Relations among stability parameters in the surface layer, Boundary-Layer Meteorology 3 (1972) 47-58.

Hall W.D. and Pruppacher H.R 1976, The survival of ice particles falling from cirrus clouds in subsaturated air. *J. Atmos. Sci.*, 33, 1995-2000

Hinds W.C. Aerosol Technology, 2nd Ed. New York: John Wiley & Sons, 1999

Hinds W.C. Physical and Chemical Changes in the Particulate Phase, Aerosol Measurements: Principles, Techniques, and Applications, Second Edition, Edited by Paul A. Baron and Klaus Willeke, 2001

Houghton H.G., A Study of the Evaporation of Small Water Drops, Physics Vol.4, pp 419-424, December 1933

Morawska L., Droplet fate in indoor environments, or can we prevent the spread of infection?, Indoor Air 2006; 16: 335–347

Kukkonen J., Vesala T. and Kulmala M., The Interdependence of Evaporation and Settling for Airborne Freely Falling Droplets ,J. Aerosol Sci., Vol. 20, No. 7, pp. 749 763, 1989.

Neumann J., Richardson's number and the Monin-Obukhov wind profile, Journal of Meteorology, vol. 18, December 1961

Pruppacher, H.R. and J.D. Klett, 1978: *Microphysics of Clouds and Precipitation*, D. Reidel Publishing Co., Dordrecht, Holland

Williams M.D., Brown M.J. and Nelson M.A. QUIC-PLUME Theory Guide (Version 5.5), March 16, 2009

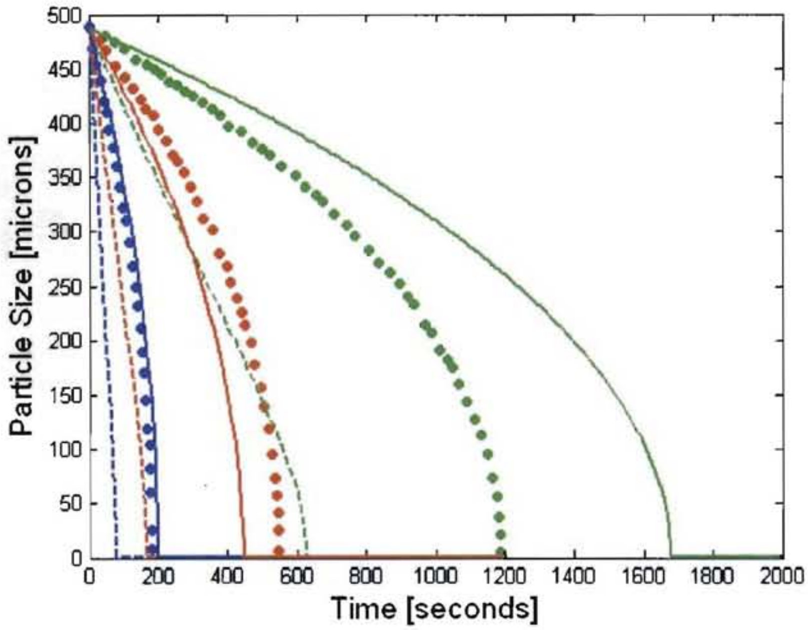

Figure1. Comparison of experimental results with QUIC Plume calculations (green RH=88% T=20.8C, red RH=53% T=19.6C, blue RH=0% T=21.7C): dots are experimental measurements, dash lines QUIC results, full lines QUIC with zero ventilation.

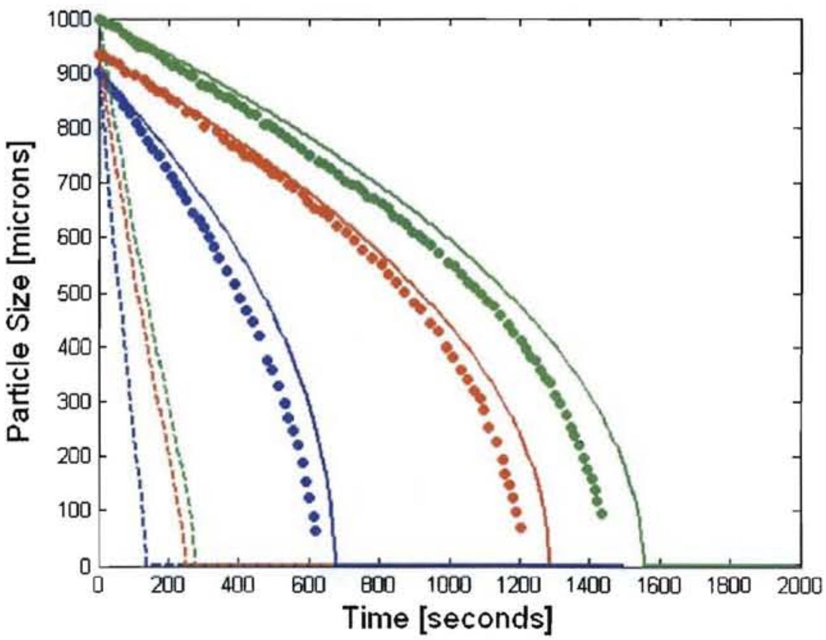

Figure 2. Comparison of experimental results with QUIC Plume calculations (Green RH=0% T=4.8C, red RH=42% T=20.3C, blue RH=0% T=22C): dots are experimental results, dash lines are QUIC results and full lines represent QUIC results with zero ventilation.

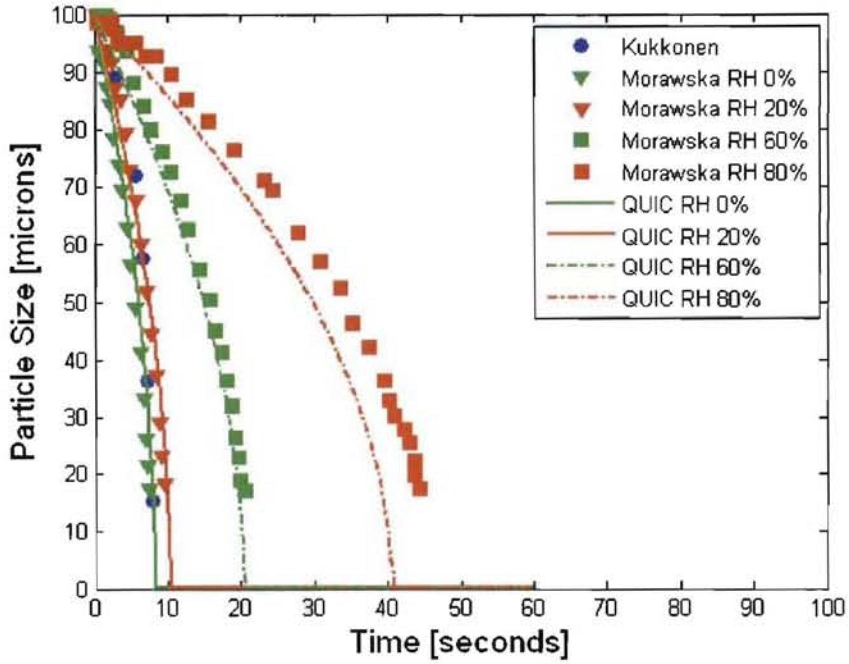

Figure 3. Comparison of QUIC Plume results with calculations of Kukkonen et.al. (1989) and Morawska 2006. Temperature set during QUIC calculations was 20 °C.

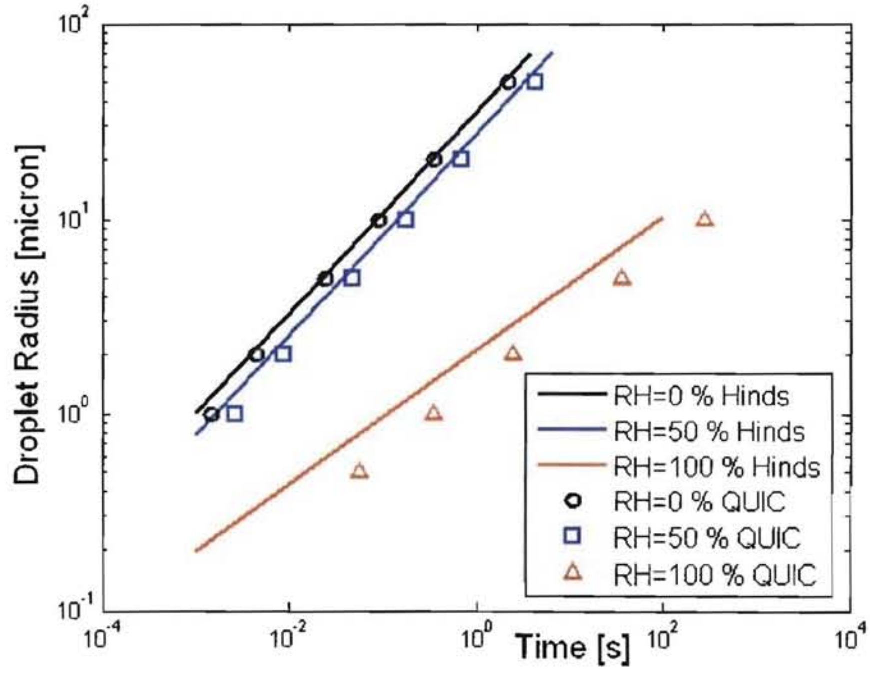

Figure 4. Comparison of drying times for different initial pure water droplet sizes at temperature 20 °C. Lines are Hinds' model results while symbols represent QUIC results.

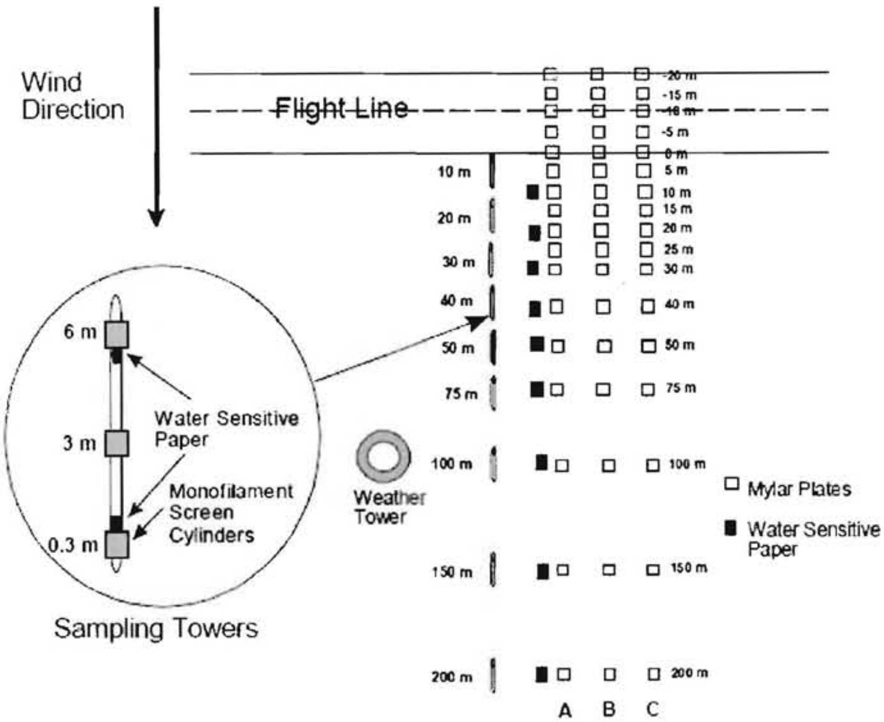

Figure 5. Field test geometry and distribution of equipment (from Fritz and Hoffmann 2007).

Rep	Time of Acquisition	Temp.at 2.5 m (°C)	Relative Humidity (%)	Wind Speed at 2.5 m (m/s)	Ri[1]
1	7:16 am	21.5	95.7	0.01	0.82
2	7:43 am	23.0	92.1	0.4	-0.77
3	8:02 am	24.2	88.7	0.9	-3.4
4	8:18 am	24.8	86.2	0.8	-717
5	8:35 am	25.8	82.7	0.9	-1.8
6	8:50 am	26.6	79.0	0.9	-22
7	7:04 pm	34.5	37.8	2.3	-0.030
8	7:20 pm	34.1	38.7	2.2	0.048
9	7:36 pm	33.5	42.1	1.9	0.081
10	7:52 pm	33.3	42.2	2.1	0.086
11	8:08 pm	32.6	44.5	2.1	0.11
12	8:24 pm	31.4	48.3	1.4	0.22

Table 1. Meteorological conditions measured and calculated during field tests (Fritz and Hoffmann 2007).

Rep	Integrated Deposition In-swath (% Applied)	Integrated Downwind Deposition 0-200 m (% Applied)
1	73	25
2	78	17
3	56	33
4	66	22
5	60	17
6	51	20
7	38	22
8	60	13
9	34	15
10	40	10
11	33	12
12	45	15

Table 2. Measured in-swath and downwind deposition.

		Downwind Distance (m)									
	Rep	0-10	10-20	20-30	30-40	40-50	50-75	75-100	100-150	150-200	Total
Incremental Deposition (% of Applied)	1	14	5.7	2	0.9	0.6	1	0.2	0.2	0.1	25
	2	10	2.2	1	0.8	0.5	0.7	0.4	0.4	0.2	17
	3	20	5.5	3.2	2	0.9	0.9	0.3	0.3	0.1	33
	4	17	2.4	0.9	0.2	0.2	0.4	0.1	0.1	0.1	22
	5	13	1.8	0.8	0.3	0.3	0.2	0.1	0.2	0.1	17
	6	15	2.9	0.9	0.5	0.3	0.2	0.1	0.1	0.1	20
	7	7.3	4.5	3.3	2.3	2.4	0.8	0.7	0.5	0.5	22
	8	7.2	2.8	0.9	0.3	0.5	0.3	0.6	0.4	0.2	13
	9	8.1	3.6	1	0.4	0.5	0.4	0.6	0.4	0.4	15
	10	4.4	2.1	0.8	0.5	0.4	0.3	0.5	0.4	0.3	10
	11	5.8	2.1	0.9	0.5	0.8	0.4	0.6	0.4	0.4	12

Table 3. Downwind deposition as a function of downwind distance.

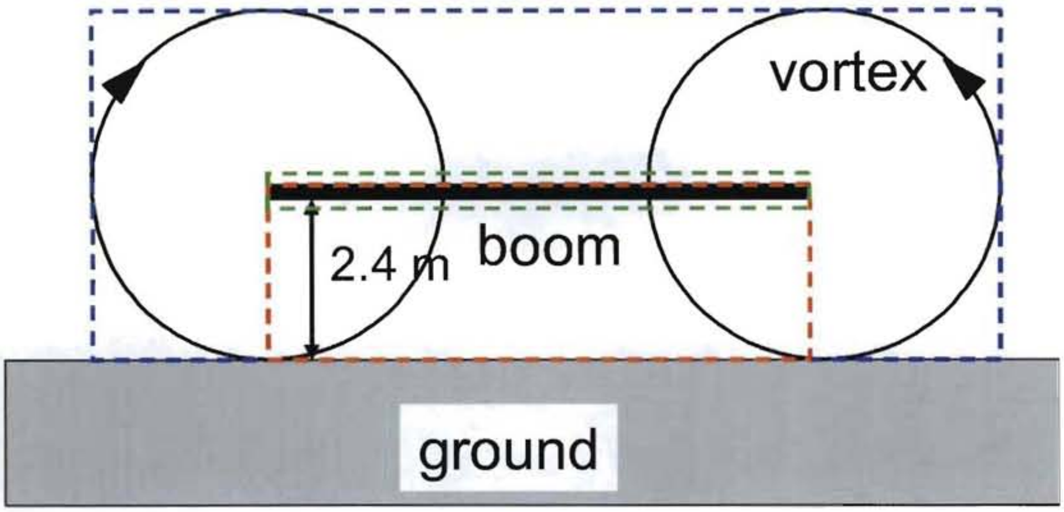

Figure 6. Geometry of sources used in QUIC simulations.

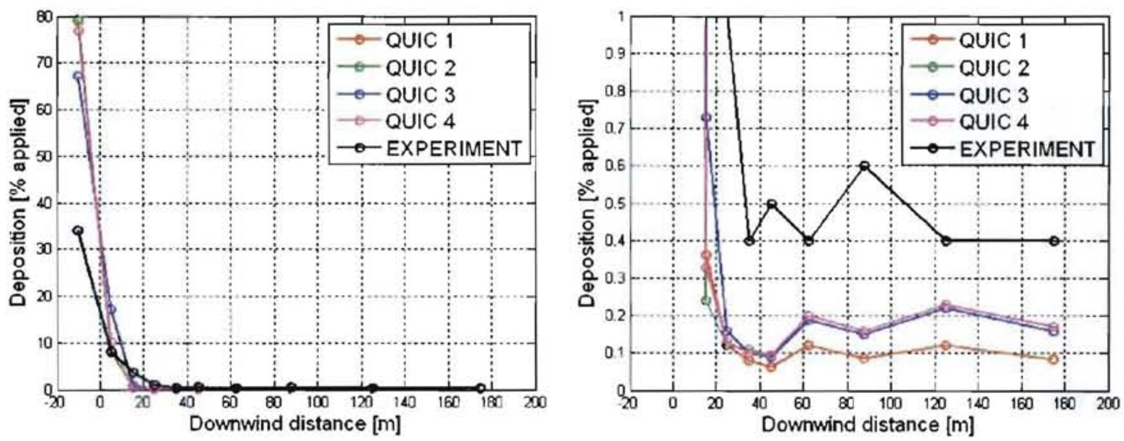

Figure 7. The comparison of experimental and model results for case 9 (1/L=0.047). The plot on the right is the same as the left one but zoomed in order to better show results of further downwind deposition. Numbers in legend (QUIC 1-4) denote QUIC runs: 1-neutral stability; 2-stable, source height 2.4 m; 3-stable, source height 4.8 m and 4-stable, thin elevated source.

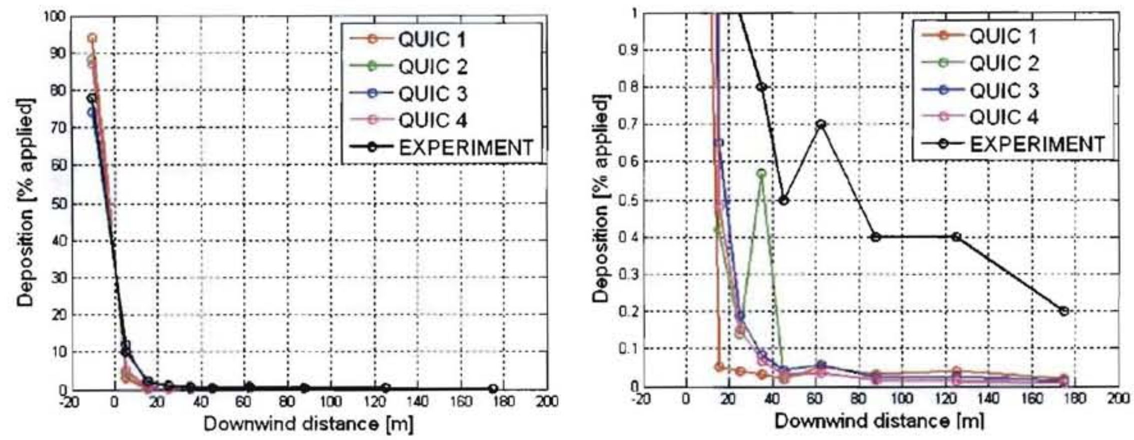

Figure 8. The comparison of experimental and model results for case 2 (1/L=-0.24). The plot on the right is the same as the left one but zoomed in order to better show results of further downwind deposition. Numbers in legend (QUIC 1-4) denote QUIC runs: 1-neutral stability; 2-unstable, source height 2.4 m; 3-unstable, source height 4.8 m and 4-unstable, thin elevated source.

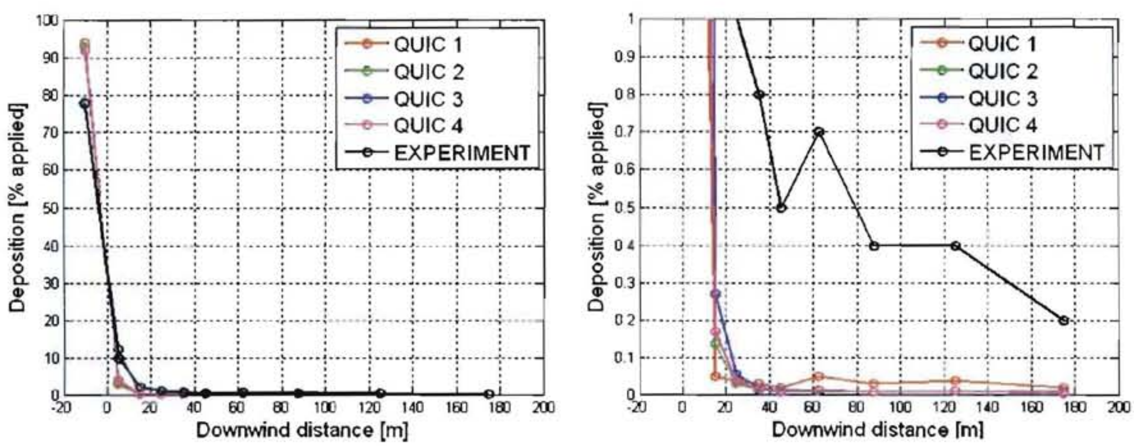

Figure 9. The comparison of experimental and model results for case 2 (1/L=-0.04). The plot on the right is the same as the left one but zoomed in order to better show results of further downwind deposition. Numbers in legend (QUIC 1-4) denote QUIC runs: 1-neutral stability; 2-unstable, source height 2.4 m; 3-unstable, source height 4.8 m and 4-unstable, thin elevated source.